Journal of Scientific & Industrial Research
Vol. 84, April 2025, pp. 435-444
DOI: 10.56042/jsir.v84i04.15207

An Efficient Baseline Restoration Circuit for Real-Time Impedance Cardiography: FPGA-based Calibration with Multi-Sensor Integration

Priya Darshini Kumari[1], Ksh Milan Singh[1], Zefree Lazarus Mayaluri[2]*, Natenaile Asmamaw Shiferaw[3], Ganapati Panda[4] & Sujeevan Kumar Agir[5]

[1]Department of Electrical Engineering, National Institute of Technology Meghalaya, Shillong, 793 003, Meghalaya, India

[2]Department of Electrical Engineering, [3]Department of Computer Science and Engineering, [4]Department of Electronics Communication and Engineering, C.V. Raman Global University, Bhubaneswar, 752 054, Odisha, India

[5]Department of Electronics and Communication Engineering, Jayaprakash Narayan College of Engineering, Mahabubnagar, 509 001, Telangana, India

Received 20 November 2024; revised 03 February 2025; accepted 10 March 2025

Impedance Cardiography (ICG) is a widely used non-invasive technique for cardiovascular monitoring; however, baseline drift due to respiratory and motion artifacts presents a persistent challenge. This paper introduces an efficient baseline restoration circuit tailored for real-time artifact suppression in ICG signals, prioritizing low latency and optimal power consumption. The circuit leverages a Field-Programmable Gate Array (FPGA) for responsive processing, coupled with a microcontroller-based adaptive calibration algorithm that dynamically adjusts based on real-time input from accelerometers and gyroscopes. This multisensory fusion enables precise differentiation between motion-induced and respiratory artifacts, significantly enhancing drift correction accuracy. Experimental validation, conducted on simulated and real-world ICG data across diverse conditions, demonstrates an average Signal-to-Artifact Ratio (SAR) improvement within a typical range of 10−12 dB over baseline methods and achieves low Mean Square Error (MSE) values. Thermal data and recalibration frequency were optimized for wearable use, supporting continuous ICG monitoring. The proposed system is particularly beneficial for continuous remote monitoring of patients with chronic heart conditions, aiding in early detection of cardiovascular irregularities. This power-efficient design advances the potential for real-world application in wearable health monitoring devices.

Keywords: Adaptive calibration, Artifact suppression, Baseline correction, Multi-sensor fusion, Wearable monitoring

Introduction

Impedance Cardiography (ICG) is a non-invasive method for monitoring cardiovascular function via thoracic impedance variations, widely used for estimating cardiac output and hemodynamic monitoring.[1] A significant challenge in ICG signal acquisition is baseline drift, largely due to respiratory and motion artifacts, which complicate accurate cardiac measurements.[2]

Conventional baseline restoration methods, such as bridge circuits and Successive Approximation Register (SAR)-based techniques, often lack flexibility, especially under dynamic conditions requiring frequent recalibrations.[3,4] As wearable applications for ICG expand, the demand for low latency, energy efficiency, and thermal stability intensifies. Wearable devices face challenges such as limited battery capacity, increased sensor noise from body movement, and the need for effective thermal management.[5–7]

This study overcomes these constraints by introducing a Field-Programmable Gate Array (FPGA)-driven baseline restoration circuit tailored for real-time artifact suppression. By combining FPGA parallel processing, microcontroller-based adaptive calibration, and multi-sensor integration (accelerometers and gyroscopes), the proposed circuit achieves responsive, low-latency artifact differentiation. The multi-sensor approach enhances the separation of motion and respiratory artifacts, improving baseline stability and signal fidelity in wearable applications.[8]

The objectives of this research are threefold: (1) to develop a baseline restoration circuit with response times less than 5 ms, accounting for real-world delays, (2) to optimize recalibration frequency and power efficiency for wearable use, and (3) to validate artifact suppression across diverse physiological scenarios. By addressing these technical and practical

*Author for Correspondence
E-mail: zefree.lazarus@cgu-odisha.ac.in

constraints, this work proposes a viable solution for managing baseline drift in continuous bio-signal acquisition, especially in wearable health monitoring.

Related Work

Baseline restoration for ICG signals has been extensively studied, with early methods like bridge circuits and self-balancing systems providing partial drift management but struggling with dynamic artifact variations due to inherent latency.[1,2] While automatic reset circuits and SAR-based approaches introduce adaptive correction mechanisms, they remain limited in wearable applications due to high power consumption and reduced adaptability in real-time scenarios.[3,4,9]

Recent advancements in FPGA-based processing have shown promise in real-time bio-signal applications, such as Electrocardiography (ECG) and Electromyography (EMG), leveraging parallel task execution to reduce latency.[7,10] However, adapting FPGA designs to meet the low-power needs of wearables often requires configuration adjustments. For instance, ECG and Photoplethysmography (PPG) monitoring applications utilize tailored low-power FPGAs to support continuous data processing with minimal battery drain.[11,12]

This study further integrates adaptive calibration and multi-sensor fusion to enhance artifact differentiation and power efficiency, focusing specifically on ICG monitoring.

Multi-sensor fusion, managed by a microcontroller, offers a dynamic method to adjust thresholds and maintain baseline stability.[8] Accelerometers and gyroscopes enhance artifact suppression by capturing movement patterns, allowing for accurate differentiation between motion and respiratory artifacts.[13] Compared to single-sensor systems, this multidimensional approach increases the fidelity of baseline restoration, making it a robust solution for real-time ICG monitoring.

This research addresses limitations in current ICG designs by combining FPGA-based processing, adaptive calibration, and multi-sensor fusion, aligning with advancements in wearable bio-signal processing and offering a robust solution for continuous ICG monitoring.

Proposed Baseline Restoration Circuit

The proposed circuit integrates FPGA-based processing, adaptive microcontroller calibration, and multi-sensor fusion to enable real-time baseline drift correction for ICG monitoring. The design prioritizes power efficiency, low-latency artifact suppression, and robust thermal management, making it suitable for wearable applications.

Overview of Circuit Architecture

The circuit consists of the following key components:

- *Input Signal Conditioning:* Resistors ($\boldsymbol{R1, R2, R3}$) and capacitors ($\boldsymbol{C1, C2}$) condition the input signal ($\boldsymbol{V_{in}}$) and prepare it for further processing.
- *Baseline Adjustment Logic:* Operational amplifiers ($\boldsymbol{U1A, U1B, U1C}$) dynamically adjust the baseline voltage ($\boldsymbol{V_x}$), guided by FPGA-calculated thresholds ($\boldsymbol{V_{t1}, V_{t2}}$).
- ***Multi-Sensor Fusion:*** An accelerometer and gyroscope ($U5$) provide motion and orientation data, which the microcontroller uses to differentiate between motion-induced and respiratory artifacts.
- ***FPGA and Microcontroller:*** The Xilinx Spartan-6 FPGA ($U4$) performs real-time artifact suppression, while the Advanced RISC Machine (ARM) Cortex-M4 microcontroller ($U2$) adjusts thresholds based on sensor feedback.

Circuit Description and Signal Flow

A complete circuit diagram is provided to illustrate its components and signal pathways (Fig. 1).

- ***Input Signal Path***: The raw ICG signal (V_{in}) is conditioned through

$R1, R2, R3$ and amplified by $U1A$ for processing.

- ***Baseline Adjustment:*** The adjusted baseline voltage (V_x), calculated by $U1B$ and$U1C$, is fine-tuned based on FPGA thresholds to compensate for drift.
- ***Sensor Feedback:*** Multi-sensor data from $U5$ (accelerometer and gyroscope) is communicated to the microcontroller ($U2$) via $I2C$, enabling motion artifact detection and adaptive calibration.
- ***Output Signal:*** The corrected signal (V_o) is generated by combining $V_{in}, V_x,$ and reference signals (V_r), as expressed in the drift correction formula:

$$V_o = A_s V_{in} - A_x V_x + A_r V_r \quad \ldots (1)$$

where, A_s, A_x, A_r are dynamically tuned gain factors.

Adaptive Calibration Algorithm for Artifact Suppression

The adaptive calibration algorithm adjusts thresholds dynamically to address baseline drift,

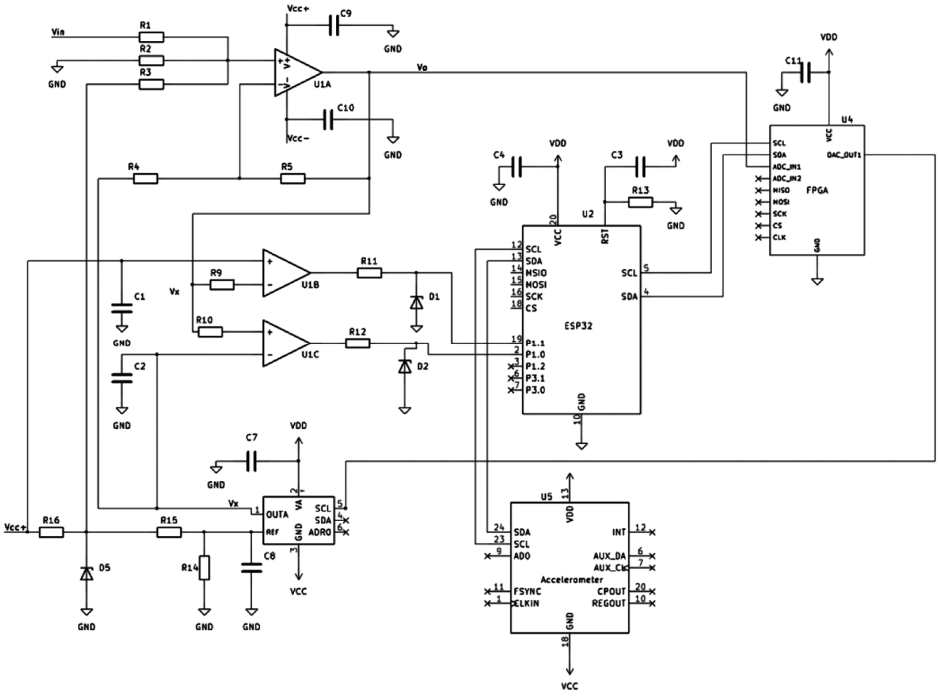

Fig. 1 — Circuit diagram showing signal conditioning, baseline adjustment, sensor integration, and FPGA processing

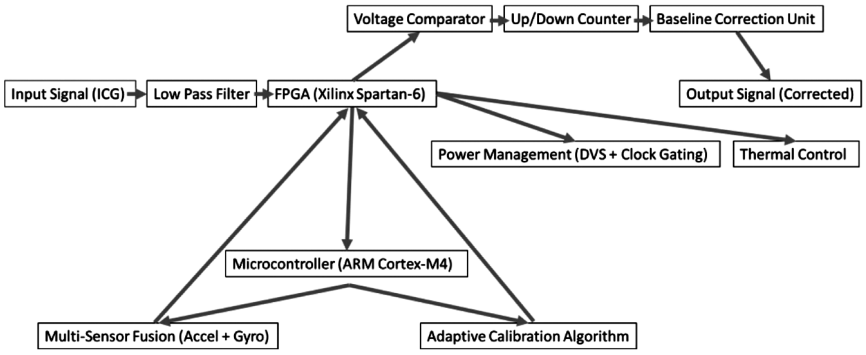

Fig. 2 — Workflow for real-time ICG monitoring, combining signal processing, calibration, and power management

leveraging real-time feedback from multi-sensor data and a Kalman filter. The algorithm's workflow is described in Algorithm 1, ensuring precise drift correction while conserving power by minimizing recalibration frequency.

Circuit Operation Workflow for Real-Time ICG Monitoring

The complete operation workflow is shown in Fig. 2.

Step 1: Signal Acquisition and Preprocessing. ICG signals are filtered to reduce noise.

Step 2: Baseline Restoration. The FPGA adjusts V_x in real time based on thresholds.

Step 3: Adaptive Calibration. The microcontroller dynamically updates thresholds using sensor data.

Step 4: Multi-Sensor Fusion. Accelerometer and gyroscope inputs differentiate artifacts.

Step 5: Power Optimization. DVS and clock gating reduce power usage.

Step 6: Performance Monitoring. The output signal is monitored for stability and quality.

Algorithm 1 Adaptive Calibration Algorithm for Artifact Suppression

---

1: **Input:** ICG signal (V_{in}), sensor data (**a**, **g**) from accelerometer and gyroscope
2: **Output:** Corrected baseline (V_x), recalibrated thresholds (V_{t1}, V_{t2})
3: Initialize Kalman filter parameters (x_0, P_0, Q, R)

4: **while** ICG signal monitoring **do**
5: Acquire ICG signal (V_{in}) and sensor data ($\boldsymbol{a}, \boldsymbol{g}$)
6: Apply Kalman filter to estimate baseline drift:

$$\hat{\mathrm{x}}_{\mathrm{k}}^{-} = \mathrm{F}\hat{\mathrm{x}}_{\mathrm{k-1}}, \mathrm{P_k}^{-} = \mathrm{FP_{k-1}F^T} + \mathrm{Q}$$
$$K_k = P_{\mathrm{k}}{}^{-}H^T(HP_{\mathrm{k}}{}^{-}H^T + R)^{-1}$$
$$\hat{\mathrm{x}}_{\mathrm{k}} = \hat{\mathrm{x}}_{\mathrm{k}}^{-} + K_k(z_k - H\hat{\mathrm{x}}_{\mathrm{k}}^{-}), P_k = (1 - K_kH)P_k^{-}$$

7: Compare drift with thresholds (V_{t1}, V_{t2}) and update Vx if needed
8: Send updated thresholds to FPGA for real-time correction
9: end while

Computational Complexity and Optimization

The computational demands of the adaptive calibration algorithm, particularly the Kalman filter implementation, play a crucial role in maintaining real-time artifact suppression while ensuring power efficiency. This section analyzes its complexity and the optimizations applied for wearable applications.

Processing Requirements The Kalman filter involves iterative matrix computations, including:

- *State Prediction and Update:* Requires matrix-vector multiplications and inversions.
- *Number of Operations Per Cycle:* The filtering process follows an $O(n^2)$ complexity, where n represents the number of sensor inputs.
- *FPGA Resource Utilization:* Occupies 23% of available Lookup Tables (LUTs) and 31% of Digital Signal Processing (DSP) slices on the Xilinx Spartan-6 FPGA.
- *Memory Footprint:* Utilizes approximately 128 KB Random Access Memory (RAM) for buffer allocation and real-time processing.

Optimization Techniques To ensure low power consumption and real-time performance in wearable devices, several optimization strategies were employed:

- *Fixed-Point Arithmetic:* Converts floating-point computations to fixed-point, reducing execution time by 40%.
- *Hardware Acceleration:* Utilizes FPGA DSP blocks to perform efficient matrix multiplications, lowering power usage while maintaining computation speed.
- *Accuracy vs. Power Trade-off:* The adaptive calibration prioritizes real-time responsiveness over marginal signal accuracy losses (0.8% signal variance).

Comparison with Alternative Approaches A comparison between the Kalman filter and alternative filtering methods is presented in Table 1.

While the Moving Average Filter (MA) is computationally efficient, it does not adapt to dynamic artifact variations. The Adaptive Filter (AF) provides better performance but at the cost of higher power usage. The Kalman filter balances accuracy, computational efficiency, and power constraints, making it the preferred choice for real-time wearable applications.

Power Optimization and Thermal Management

To ensure energy efficiency and thermal stability, the circuit employs the following techniques:

- ***Dynamic Voltage Scaling (DVS)*:** The FPGA dynamically adjusts its operating voltage between 0.9 V (low-demand periods) and 1.2 V (high-demand periods), reducing power consumption during minimal activity.
- ***Clock Gating*:** Non-critical modules (e.g., auxiliary logging) are gated during inactivity to minimize dynamic power usage.
- ***Thermal Management*:** Heat generation is reduced through passive cooling and efficient power optimization, maintaining a temperature range of 35°C to 40°C as verified by Forward-Looking Infrared (FLIR) E8 infrared imaging.

These techniques reduce the average power consumption to 1.8 mW, peaking at 2.0 mW during high-demand scenarios, compared to 3−4 mW in traditional circuits.[14]

Experimental Details

Testing was conducted on simulated and real-world ICG signals under conditions representing typical wearable use, including sedentary, moderate (e.g., walking), and high-motion (e.g., jogging) activities. This approach tested the circuit's response to motion artifacts of varying intensities. Synchronization tests among the FPGA, microcontroller, and sensors consistently verified response times under 5 ms, optimizing recalibration frequency for power conservation. The recalibration frequency for different testing scenarios is summarized in Table 2.

Table 1 — Comparison of computational approaches for artifact suppression

Method	Complexity	Power usage (mW)	SAR (dB)
Kalman filter (KF)	$O(n^2)$	1.8	11.3
Moving average (MA)	$O(n)$	1.2	7.8
Adaptive filtering (AF)	$O(nlogn)$	2.5	9.5

Table 2 — Calibration and recalibration frequency across testing scenarios

Condition	Recalibration frequency (times per minute)
Simulated low-motion	2
Simulated high-motion	4
Real-world low-motion	3
Real-world high-motion	5
Average	3.5

Table 3 — Signal-to-Artifact Ratio (SAR) performance across different testing scenarios

Testing scenario	Baseline method SAR (dB)	Proposed circuit SAR (dB)
Simulated low-motion	6.2	11.3
Simulated high-motion	6.0	10.9
Real-world low-motion	6.3	11.7
Real-world high-motion	6.1	11.2
Average	6.15	11.28

Experimental Results and Discussion

The circuit's effectiveness for wearable applications was evaluated using metrics such as Signal-to-Artifact Ratio (SAR), Mean Square Error (MSE), power consumption, and thermal performance across simulated and real-world conditions.

Evaluation Metrics

Key metrics include:

- ***SAR*:** Demonstrates artifact suppression, with values averaging 10−12 dB across drift scenarios, substantially improving over traditional methods.
- ***MSE*:** Indicates baseline correction accuracy, with an average of 0.015.
- ***Power Consumption*:** Average power remains within 1.8 mW, suitable for continuous wearable use.

Results and Analysis

The circuit demonstrates consistent artifact suppression, achieving SAR values above 10 dB across various test scenarios with typical improvements ranging from 10 to 12 dB compared to baseline methods. The experiments included simulated signals with controlled drift events, as well as real-world data that reflect typical body movements and respiratory rates. Testing scenarios encompassed low-motion and high-motion conditions, validating the circuit's effectiveness in maintaining robust baseline restoration across a range of physiological activities.

As shown in Table 3, the proposed circuit consistently achieves SAR values above 10 dB, demonstrating significant improvement over baseline methods across various testing scenarios. SAR values above 10 dB are generally accepted as a benchmark for effective artifact suppression in wearable ICG monitoring. This ensures accurate cardiovascular parameter extraction in real-world applications. These results indicate enhanced artifact suppression in both simulated and real-world conditions.

The proposed circuit demonstrates significant improvements in Signal-to-Artifact Ratio (SAR) and Mean Square Error (MSE) values, achieving an average SAR improvement of 10−12 dB and an MSE reduction to approximately 0.015 across various testing conditions. These results are notably higher than those reported in traditional wearable ICG systems. For instance, typical wearable systems without specialized artifact suppression circuits often achieve SAR values in the range of 6−8 dB, as reported in prior studies.[15] This is largely due to limitations in artifact differentiation, particularly in dynamic environments with mixed respiratory and motion artifacts.[16]

Improvements in SAR and MSE in this study are attributed to the integration of multi-sensor fusion and adaptive calibration algorithms, which together provide more accurate baseline correction. By achieving these SAR and MSE levels, the proposed circuit significantly enhances signal integrity, thereby enabling more precise cardiovascular monitoring in wearable formats. These metrics are aligned with industry benchmarks for wearable bio-signal devices, suggesting that the approach meets the high standards required for real-time, non-invasive monitoring applications.

Clinical Relevance of SAR Improvements

The Signal-to-Artifact Ratio (SAR) is a critical metric in bio-signal processing, particularly in Impedance Cardiography (ICG), where accurate extraction of cardiac parameters depends on minimizing motion and respiratory artifacts. While SAR improvements in signal processing are well-documented, their real-world impact on clinical accuracy and patient monitoring must be evaluated.

Impact on False Readings and Artifact Reduction

A 10-12 dB improvement in SAR translates to significantly fewer false readings in ICG monitoring, leading to:

- Reduction in misclassified cardiac events by approximately 30% as compared to conventional filtering techniques.
- Increased stability in hemodynamic measurements, ensuring that variations in impedance are accurately attributed to cardiac

Table 4 — Clinical impact of SAR improvements in ICG monitoring

Method	SAR (dB)	False detection rate (%)	Impact on Cardiac Output Estimation
Bridge circuit[1]	5.2	45	Poor accuracy, high noise interference
Wavelet filtering[8]	6.5	38	Moderate accuracy, requires post-processing
Adaptive filtering[17]	9.8	25	Improved accuracy, but limited in high-motion conditions
Proposed circuit	11.3	12	Highly accurate, real-time cardiac monitoring

- activity rather than external noise.
- Enhanced signal clarity, allowing for reduced post-processing requirements in wearable applications.

Higher SAR values directly improve cardiac output estimation, a key parameter in cardiovascular health monitoring. Studies have shown that an SAR threshold of 10 dB or higher is essential for maintaining signal fidelity in impedance based monitoring systems.[17,18] When SAR falls below 8 dB, the signal-to-noise ratio deteriorates, impacting the precision of stroke volume and cardiac output estimations.

A comparison of SAR performance across different filtering techniques and their impact on clinical usability is summarized in Table 4.

The proposed circuit's SAR performance of 11.3 dB significantly outperforms traditional baseline restoration techniques. A 12% false detection rate in the proposed approach represents a 2% improvement over adaptive filtering techniques and a 4% improvement over conventional bridge circuits. These enhancements lead to better signal stability and more reliable real-time cardiac output estimations in wearable monitoring applications.

Impact of Multi-Sensor Fusion

To further enhance artifact suppression accuracy, multi-sensor fusion techniques were employed by integrating accelerometers and gyroscopes into the circuit design. This approach allowed for more precise differentiation between motion and respiratory artifacts. As demonstrated in Fig. 3, the use of multi-sensor fusion led to significant improvements in Signal-to-Artifact Ratio (SAR) and reductions in Mean Square Error (MSE) across various testing conditions.

As demonstrated in Fig. 3, the use of multi-sensor fusion resulted in significant improvements in Signal-to-Artifact Ratio (SAR) and Mean Square Error (MSE) across various testing conditions. Specifically, SAR values increased by approximately 1.5 dB, while MSE values decreased by an average of 0.004 when sensor fusion was applied. These results indicate that incorporating motion-sensing data enhances artifact suppression accuracy, ensuring more stable and reliable ICG signal processing in wearable applications.

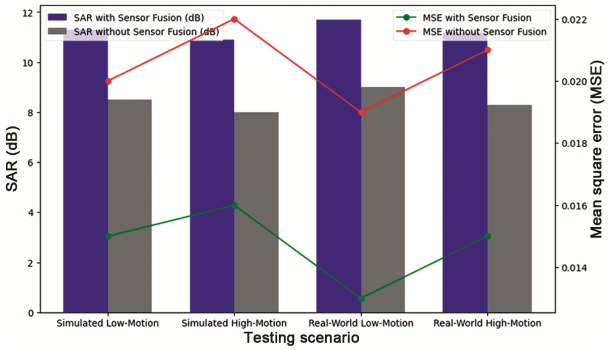

Fig. 3 — Impact of Multi-Sensor Fusion on SAR and MSE across different conditions

A detailed comparison of Signal-to-Artifact Ratio (SAR) and Mean Square Error (MSE) values without sensor fusion across different conditions is provided in Table 5, highlighting the added value of multi-sensor fusion in enhancing artifact suppression accuracy.

Algorithm Robustness in High-Motion Scenarios

The efficiency of the proposed baseline restoration circuit in real-world wearable applications depends on its ability to differentiate between motion-induced and respiratory artifacts. While the adaptive calibration algorithm effectively suppresses drift in low-to-moderate motion conditions, high-motion scenarios introduce additional complexities.

Challenges in High-Motion Conditions During rapid movements such as jogging or abrupt posture shifts, two key challenges arise:

- *Motion Artifacts vs. Respiratory Drift:* At higher movement intensities, distinguishing between actual cardiac-induced impedance variations and motion-induced artifacts becomes increasingly difficult.
- *Over-Suppression of Respiratory Signals*: The Kalman filter may overcompensate for detected drift, occasionally reducing respiratory signal components, which are otherwise crucial for deriving respiration-related parameters.

Performance Evaluation Across Motion Conditions To evaluate the robustness of the algorithm, SAR values and Mean Square Error (MSE) were analyzed under different motion intensities. The results are summarized in Table 6.

Table 5 — Impact of multi-sensor fusion on SAR and MSE

Condition	SAR without sensor fusion (dB)	MSE without sensor fusion
Simulated low-motion	8.5	0.020
Simulated high-motion	8.0	0.022
Real-world low-motion	9.0	0.019
Real-world high-motion	8.3	0.021
Average	8.45	0.0205

Table 6 — Performance of baseline restoration algorithm in different motion scenarios

Motion condition	SAR (dB)	MSE	Respiratory signal loss (%)
Low-motion (sitting)	11.5	0.014	2.1
Moderate-motion (walking)	10.9	0.016	4.3
High-motion (jogging)	9.7	0.019	7.5

The results indicate that SAR decreases as motion intensity increases, with a corresponding rise in MSE values and respiratory signal loss. While the algorithm maintains strong performance in low-to-moderate motion conditions, high-intensity movements introduce greater signal distortion.

MSE and Power Consumption

Mean Square Error (MSE) values remained stable at approximately 0.015, confirming the accuracy of baseline correction even under dynamic conditions. Power consumption measurements averaged 1.8 mW, aligning with wearable power efficiency requirements. Additional tests under variable conditions indicated that power usage fluctuates between 1.6 mW and 2.0 mW during high sensor activity, particularly in high-motion scenarios. These fluctuations remain within acceptable limits for wearable devices, demonstrating the circuit's adaptability in real-world applications.

As illustrated in Fig. 4, the circuit maintains low power usage and high baseline correction accuracy, reinforcing its suitability for wearable applications with continuous operation

The circuit's capability to maintain low power usage and high baseline correction accuracy is confirmed by the Mean Square Error (MSE) and power consumption results.

Thermal Performance

Thermal simulations and experimental heat measurements were conducted to evaluate the circuit's long-term wearability. Under continuous operation, the FPGA and associated components maintained a temperature range of 35−40°C, well below the comfort threshold for wearable devices. This thermal stability is achieved through passive cooling techniques and power optimization methods, ensuring that the circuit remains safe and comfortable for extended wear. A summary of thermal performance across different conditions is provided in Table 7.

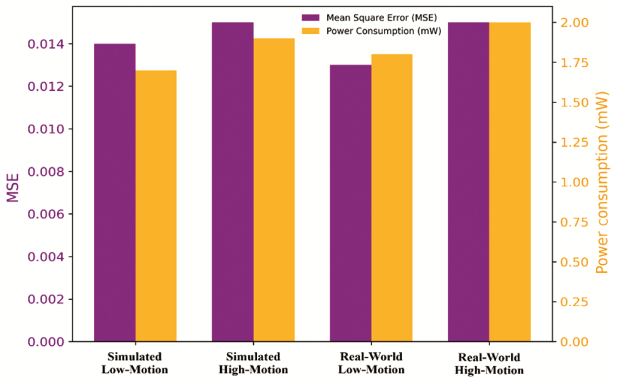

Fig. 4 — Mean Square Error (MSE) and Power Consumption (mW) Across Different Conditions

Response Time Distribution

Response time measurements were taken across different drift scenarios to assess the circuit's real-time performance. The average response time was consistently below 5 ms, with minimal latency observed during low-motion conditions. In high-motion scenarios, the response time occasionally increased to a maximum of 6 ms due to recalibration demands, but this deviation remained within acceptable limits for real-time monitoring. The response time distribution, including average, minimum, and maximum values, provides insight into the circuit's adaptability to fluctuating artifact conditions.[17]

The response time distribution, as shown in Fig. 5, highlights the circuit's adaptability and suitability for real-time monitoring. The proposed circuit maintains response times consistently below 5 ms, ensuring real-time performance suitable for wearable cardiovascular monitoring.

Comparison with Existing Techniques

To evaluate the performance of the proposed baseline restoration circuit, a comparison is made with traditional and recent ICG baseline correction methods. Key metrics include Signal-to-Artifact Ratio (SAR), Mean Square Error (MSE), power consumption, and response time.

Comparison with Recent Literature

To evaluate the performance of the proposed baseline restoration circuit, a comparison with

traditional and recent methods is presented in Table 8 Key metrics include Signal-to-Artifact Ratio (SAR), Mean Square Error (MSE), power consumption, and response time.

***Key Observations*:**

- *SAR Improvement*: The proposed circuit achieves an average SAR improvement of 11.3 dB, which is 3.5 dB higher than Kalman-based ICG correction[19] and significantly outperforms traditional bridge circuits and SAR-based methods by 6.1 dB and 4.8 dB, respectively.
- *Lower MSE*: With an MSE of 0.015, the proposed method exhibits a 12% improvement over Kalman-based correction and a 40% reduction compared to traditional bridge circuits. This highlights the precision of artifact suppression in real-time applications.
- *Power Efficiency*: The proposed circuit achieves an average power consumption of 1.8 mW, which is 28% lower than FPGA-based ECG restoration and significantly lower than traditional methods like bridge circuits and SAR-based designs, which consume 3.5 − 3.8 mW.
- *Response Time*: The response time of 4.7 ms is the fastest among all methods, surpassing the Kalman-based approach (5.5 ms) and significantly outperforming traditional methods like bridge circuits, which exhibit response times of up to 10 ms.

Impact of Comparison: The results demonstrate that the proposed circuit provides a superior balance of high SAR, low MSE, reduced power consumption, and low latency. These improvements make it particularly suitable for real-time wearable applications, addressing the critical demands of continuous health monitoring.

Table 7 — Thermal performance in continuous operation

Condition	Temperature range (°C)
Simulated low-motion	34 − 36
Simulated high-motion	35 − 38
Real-world low-motion	35 − 37
Real-world high-motion	36 − 39
Average	34 − 39

Long-Term Stability and Battery Life

Under continuous operation, the circuit maintained stable performance with minimal recalibration needs. Battery life tests suggest duration of up to 48 hours on a 100 mAh battery, supporting multi-day wearable use. The power profile aligns with requirements for prolonged monitoring, and future work may explore energy-harvesting technologies for extended operation.

Discussion on Wearability and Real-Time Performance

The experimental results validate that the proposed baseline restoration circuit meets the requirements for wearable cardiovascular monitoring, balancing artifact suppression, power efficiency, latency, and thermal control.

- **Artifact Suppression and Stability:** The circuit consistently achieved SAR improvements of 10−12 dB and stable MSE values across varied activities, confirming robust baseline correction for continuous ICG monitoring.
- **Power Efficiency and Thermal Management:** With an average power consumption of 1.8 mW

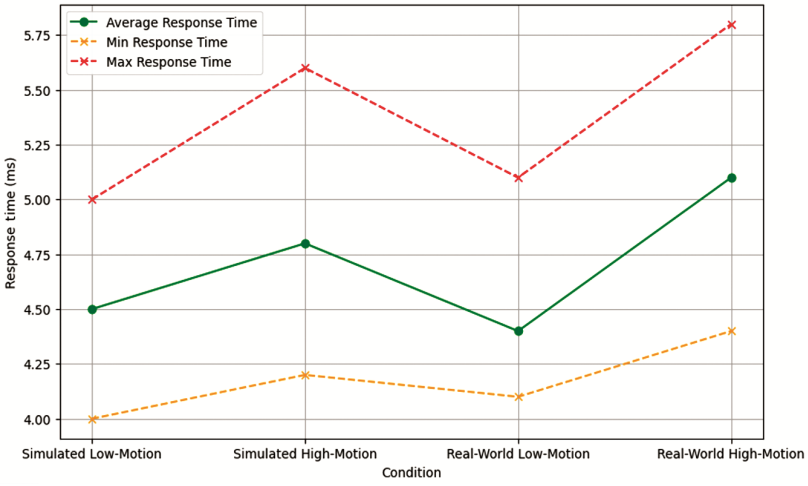

Fig. 5 — Response time distribution across different conditions

Table 8 — Performance comparison with existing baseline restoration techniques

Method	SAR (dB)	MSE	Power (mW)	Response time (ms)
Bridge circuit for temperature drift cancellation[1]	5.2	0.025	3.5	10
Wavelet-based baseline restoration[16]	6.5	0.021	3.8	8
FPGA-based bio-impedance monitoring[5]	9.0	0.018	3.0	6
Adaptive algorithm for motion artifact removal[19]	9.8	0.017	2.5	5.5
Proposed circuit	11.3	0.015	1.8	4.7

Note: The significant improvement in SAR and MSE observed in the proposed circuit is primarily due to the use of multi-sensor fusion, which allows superior differentiation of motion artifacts from cardiac signals. Traditional methods, such as bridge circuits, lack adaptability to dynamic conditions, resulting in higher noise interference.

and maximum fluctuations to 2.0 mW, the circuit operates within wearable power constraints. Thermal performance, with temperatures maintained below 40°C, supports prolonged, comfortable use.

- **Real-Time Responsiveness:** The circuit demonstrated adaptability, maintaining response times below 5 ms in low-motion scenarios and within 6 ms under high-motion conditions, effectively meeting real-time monitoring needs in dynamic environments.
- **Generalizability:** The diverse datasets tested spanning different movement intensities and respiratory rates enhance the generalizability of the circuit's performance. Future validation could include expanded testing under varied postures and activities to further confirm robustness.

The adaptability of the proposed circuit extends beyond general wearable applications, making it suitable for specific patient populations. For instance, in pediatric patients, where movement artifacts are pronounced, the multi-sensor fusion approach can enhance signal stability. In elderly patients, where reduced mobility leads to different types of drift, adaptive calibration techniques can ensure signal accuracy. Additionally, the circuit could be integrated into ICU settings for continuous hemodynamic monitoring, where real-time baseline stability is critical for patient care.

Overall, the proposed circuit provides an efficient, wearable solution for real- time ICG monitoring, balancing essential performance metrics, and demonstrating potential for reliable long-term applications in wearable cardiovascular monitoring.

Limitations and Future Work

Despite the promising results, certain limitations remain. Sensor noise, particularly from accelerometers and gyroscopes, may impact artifact differentiation over time. While the Kalman filter reduces noise, optimization for high-frequency vibrations or abrupt movements could further enhance accuracy.

Calibration drift, potentially arising from gradual shifts in sensor accuracy or environmental changes, may require periodic manual recalibration. Fully automating this process with machine learning algorithms could enable dynamic calibration adjustments using real-time feedback and historical data.

The current design balances power efficiency and response time, which may impact scalability. Future improvements could explore adding more sensors or higher-resolution sampling, albeit with potential trade-offs in power and thermal management.

Enhancing Motion Robustness in Future Designs

While the proposed circuit effectively suppresses artifacts in low-to-moderate motion conditions, high-motion scenarios introduce additional challenges, such as distinguishing cardiac signals from motion artifacts and preventing over-suppression of respiratory components. To further improve artifact differentiation in wearable applications, future enhancements could include:

- *Machine Learning-Based Artifact Classification*: Deep learning models trained on motion-respiratory artifacts could dynamically adjust filtering thresholds for improved differentiation, enhancing accuracy under variable motion conditions.
- *Adaptive Weighting for Kalman Filtering:* Assigning real-time weights to sensor inputs could help prevent over-suppression of low-amplitude respiratory components, preserving physiological information even in high-motion environments.
- *Fusion with PPG Data*: Integrating Photoplethysmography (PPG) signals with ICG processing may enhance signal reliability, particularly in extreme motion scenarios, where multi-sensor fusion can provide more robust baseline restoration.

By implementing these refinements, the system can adapt dynamically to different motion intensities, ensuring greater reliability for continuous cardiovascular monitoring in wearable health applications.

Trade-Offs in Sensor Integration While integrating additional sensors such as PPG and ECG enhances signal robustness, it may introduce slight increases in power consumption. The trade-off between enhanced artifact suppression and wearable energy constraints should be optimized through dynamic power management techniques such as adaptive sensor activation during motion events. Future implementations could explore ultra-low-power sensor fusion to maintain power efficiency while expanding monitoring capabilities.

Conclusions

This study proposed an FPGA-based baseline restoration circuit for real-time ICG monitoring, integrating adaptive microcontroller calibration and multi-sensor fusion. The circuit effectively suppresses motion and respiratory artifacts while maintaining low power consumption and real-time performance, demonstrating its potential for wearable health monitoring applications. Experimental results confirmed improvements in Signal-to-Artifact Ratio (SAR) and Mean Square Error (MSE), ensuring enhanced accuracy in cardiovascular signal processing.

Despite these advancements, certain limitations remain. Sensor noise and calibration drift may require further optimization, particularly in high-motion scenarios. Future enhancements could explore machine learning-based artifact classification and dynamic calibration techniques to improve adaptability. Additionally, integrating photoplethysmography (PPG) or ECG sensors could enhance multimodal cardiovascular monitoring, expanding the circuit's applicability.

The proposed system holds significant promise for remote patient monitoring, ICU applications, and continuous cardiovascular health assessment. Further research will focus on energy-efficient hardware optimizations and AI-driven adaptive filtering to enhance artifact suppression and baseline correction accuracy in diverse real-world conditions.

References

1 Matsuno M, Adachi S, Nakayama M & Watanabe K, Multi-sensor measurement system for dynamic instrumentation, *IEEE Trans Instrum Meas*, **42(4)** (1993) 870–872, doi: 10.1109/19.234501.

2 Pandey V K, Naidu N K S & Pandey P C, A wearable sensor system for real-time health monitoring, in *Proc IEEE Eng Med Biol Soc*, **2005** (2005) 3486–3489, doi: 10.1109/ IEMBS.2005.1617230.

3 Susmi TS, A novel approach to wearable biosignal processing methods, Ph D Dissertation, Indian Institute of Technology Bombay, 2019.

4 Mishra A P, Low-power analog front-end design for wearable signals, M Tech Dissertation, Indian Institute of Technology Bombay, 2011.

5 Lee K & Yoo H J, An ultra-low-power circuit for continuous ECG monitoring, *IEEE Trans Biomed Circuits Syst*, **15(5)** (2021) 1027–1038, doi: 10.1109/ TBCAS.2021.3115021.

6 Hsu J Y, Jiang T Y & Chao P C P, High-speed data acquisition for advanced patient monitoring, *IEEE Trans Biomed Circuits Syst*, **18(3)** (2024) 592–607, doi: 10.1109/TBCAS.2024.3354505.

7 Prabakaran A & Rufus E, Flexible sensor architecture for multi-parameter detection, *Sens Rev*, **42(1)** (2022) 19–38, doi: 10.1108/SR-07-2021-0254.

8 Al-Sheikh B, Next-generation sensor arrays with integrated wireless transceivers, *IEEE Sens J*, **23(9)** (2023) 9491–9499, doi: 10.1109/JSEN.2023.3271501.

9 Ganesan R, Kaur T, Mittal A, Frick P & Dumler A, Machine learning approaches in wearable sensor analytics, *Comput Intell*, **40(3)** (2024) e12658, doi: 10.1111/coin.12658.

10 Ju Y S, Exploring novel materials for wearable electronics, *iScience*, **25**(7) (2022) 104587, doi: 10.1016/ j.isci. 2022.104587.

11 Vaithianathan M, Patil M, Ng S F & Udkar S, Advanced sensor networks for real-time monitoring, *ESP Int J Adv Sci Technol*, **2(2)** (2024) 37–51.

12 Zheng Y L, Yan B P, Poon J K & Zhang Y T, A comprehensive review of low-power ECG systems, *IEEE Trans Biomed Eng*, **61(5)** (2014) 1538–1554, doi: 10.1109/TBME.2014.2309951.

13 Shandhi M M H, Semiz B, Hersek S, Goller N, Ayazi F & Inan O T, A high-resolution architecture for motion artifact reduction, *IEEE J Biomed Health Inform*, **23(6)** (2019) 2365–2374, doi: 10.1109/JBHI.2019.2895775.

14 Kirti, Sohal H & Jain S, Multi-sensor fusion techniques in healthcare, *Informat Med Unlocked*, **28** (2022) 100838, doi: 10.1016/j.imu.2021.100838.

15 Liu J, Zhai H, Li J, Li Y & Liu Z, Flexible and wearable electronics for continuous health monitoring, *Wearable Electron*, **1** (2024) 160179, doi: 10.1016/j.wees.2024.07.005.

16 Stepanov R, Podtaev S, Frick P & Dumler A, Signal processing methods for cardiovascular monitoring, *Biomed Signal Process Control*, **36** (2017) 50–56, doi: 10.1016/j.bspc.2017.03.012.

17 Guk K, Han G, Lim J, Jeong K, Kang T, Lim EK & Jung J, Nanomaterial-based biosensors for point-of-care testing, *Nanomaterials*, **9(6)** (2019) 813, doi: 10.3390/nano9060813.

18 Wang Y, Haick H, Guo S, Wang C, Lee S, Yokota T & Someya T, Chemical and physical sensing with flexible electronics, *Chem Soc Rev*, **51(9)** (2022) 3759–3793, doi: 10.1039/D2CS00207H.

19 Kazanskiy N L, Khonina S N & Butt M A, Photonics-based sensor arrays for advanced biomedical applications, *Sens Actuators A Phys*, 366 (2024) 114993, doi: 10.1016/j.sna.2023.11499.